Inorganic Chemistry
Article

Inorg. Chem. **2010**, *49*, 7549–7557 **7549**
DOI: 10.1021/ic101057e

Magnetic Properties of Dysprosium Cubanes Dictated by the M−O−M Angles of the $[Dy_4(\mu_3\text{-}OH)_4]$ Core

Hongshan Ke,[†,‡] Patrick Gamez,[*,§] Lang Zhao,[†] Gong-Feng Xu,[†] Shufang Xue,[†,‡] and Jinkui Tang[*,†]

[†]*Contribution from State Key Laboratory of Rare Earth Resource Utilization, Changchun Institute of Applied Chemistry, Chinese Academy of Sciences, Changchun 130022, P.R. China,* [‡]*Graduate School of the Chinese Academy of Sciences, Beijing, 100039, P.R. China, and* [§]*Leiden Institute of Chemistry, Gorlaeus Laboratories, Leiden University, PO Box 9502, 2300 RA Leiden, The Netherlands, and ICREA, Departament de Química Inorgànica, Universitat de Barcelona, Spain*

Received May 25, 2010

Two new dysprosium(III) coordination compounds, namely, $[Dy_4(\mathbf{HL})_4(C_6H_4NH_2COO)_2(\mu_3\text{-}OH)_4(\mu\text{-}OH)_2(H_2O)_4]\cdot 4CH_3CN\cdot 12H_2O$ (**1**) and $Dy_8(\mathbf{HL})_{10}(C_6H_4NH_2COO)_2(\mu_3\text{-}OH)_8(OH)_2(NO_3)_2(H_2O)_4]$ (**2**), have been synthesized from the Schiff-base ligand 2-{[(2-hydroxy-3-methoxyphenyl)methylidene]amino}benzoic acid ($\mathbf{H_2L}$) and dysprosium chloride (**1**) or dysprosium nitrate (**2**). Single-crystal X-ray diffraction studies reveal that compound **1** exhibits a tetranuclear cubane-like structure and that **2** is an octanuclear, bis-cubane complex. The $[Dy_4(\mu_3\text{-}OH)_4]$ cubane cores of **1** and **2** are structurally related; however, the magnetic properties of **1** and **2** are drastically different. Indeed, **2** shows slow relaxation of magnetization while no out-of-phase alternating current (ac) signal is noticed for **1**. These significant disparities are most likely due to the different M−O−M angles observed for the respective cubane cores.

Introduction

The observation of slow relaxation of magnetization in metal clusters is of great interest, both from a fundamental point of view[1−5] and for the potential practical applications in data storage and processing.[2,6−11] Since the early 2000s, great research efforts have been dedicated to the design and preparation of discrete magnetic clusters[12−16] because paramagnetic clusters with large-spin ground states may behave as single-molecule magnets (SMMs).[17−19] Thus, since the discovery 20 years ago of the first SMM based on manganese(III) ions,[5] various coordination compounds exhibiting this property have been described in the literature, most of them from 3d metal centers.[14,20−23] 4f-Based clusters are promising compounds for the development of high-barrier SMMs. However, the promotion of magnetic-exchange interactions between lanthanide (Ln) ions through the overlap of bridging ligand orbitals with their "contracted" 4f orbitals is a difficult task.[16] Overcoming this obstacle and promoting ferromagnetic

*To whom correspondence should be addressed. E-mail: tang@ciac.jl.cn (J.T.), patrick.gamez@qi.ub.es (P.G.).

(1) Sessoli, R.; Gatteschi, D.; Caneschi, A.; Novak, M. A. *Nature* **1993**, *365*, 141–143.
(2) Sessoli, R.; Tsai, H. L.; Schake, A. R.; Wang, S. Y.; Vincent, J. B.; Folting, K.; Gatteschi, D.; Christou, G.; Hendrickson, D. N. *J. Am. Chem. Soc.* **1993**, *115*, 1804–1816.
(3) Boskovic, C.; Wernsdorfer, W.; Folting, K.; Huffman, J. C.; Hendrickson, D. N.; Christou, G. *Inorg. Chem.* **2002**, *41*, 5107–5118.
(4) Jones, L. F.; Brechin, E. K.; Collison, D.; Harrison, A.; Teat, S. J.; Wernsdorfer, W. *Chem. Commun.* **2002**, 2974–2975.
(5) Caneschi, A.; Gatteschi, D.; Sessoli, R.; Barra, A. L.; Brunel, L. C.; Guillot, M. *J. Am. Chem. Soc.* **1991**, *113*, 5873–5874.
(6) Gatteschi, D.; Caneschi, A.; Pardi, L.; Sessoli, R. *Science* **1994**, *265*, 1054–1058.
(7) Roch, N.; Florens, S.; Bouchiat, V.; Wernsdorfer, W.; Balestro, F. *Nature* **2008**, *453*, 633–637.
(8) Wernsdorfer, W.; Sessoli, R. *Science* **1999**, *284*, 133–135.
(9) Cavallini, M.; Facchini, M.; Albonetti, C.; Biscarini, F. *Phys. Chem. Chem. Phys.* **2008**, *10*, 784–793.
(10) Leuenberger, M. N.; Loss, D. *Nature* **2001**, *410*, 789–793.
(11) Wernsdorfer, W. *Int. J. Nanotechnol.* **2010**, *7*, 497–522.
(12) Winpenny, R. E. P. *J. Chem. Soc., Dalton Trans.* **2002**, 1–10.
(13) Brechin, E. K. *Chem. Commun.* **2005**, 5141–5153.
(14) Aromi, G.; Brechin, E. K. Synthesis of 3d metallic single-molecule magnets. In *Single-Molecule Magnets and Related Phenomena*; Springer-Verlag: Berlin, Germany, 2006; Vol. *122*, pp 1−67.
(15) Thompson, L. K.; Waldmann, O.; Xu, Z. Q. *Coord. Chem. Rev.* **2005**, *249*, 2677–2690.
(16) Sessoli, R.; Powell, A. K. *Coord. Chem. Rev.* **2009**, *253*, 2328–2341.
(17) Mertes, K. M.; Suzuki, Y.; Sarachik, M. P.; Myasoedov, Y.; Shtrikman, H.; Zeldov, E.; Rumberger, E. M.; Hendrickson, D. N.; Christou, G. *Solid State Commun.* **2003**, *127*, 131–139.
(18) Gatteschi, D.; Sessoli, R.; Cornia, A. *Chem. Commun.* **2000**, 725–732.
(19) Caneschi, A.; Gatteschi, D.; Sangregorio, C.; Sessoli, R.; Sorace, L.; Cornia, A.; Novak, M. A.; Paulsen, C.; Wernsdorfer, W. *J. Magn. Magn. Mater.* **1999**, *200*, 182–201.
(20) Cadiou, C.; Murrie, M.; Paulsen, C.; Villar, V.; Wernsdorfer, W.; Winpenny, R. E. P. *Chem. Commun.* **2001**, 2666–2667.
(21) Barra, A. L.; Caneschi, A.; Cornia, A.; de Biani, F. F.; Gatteschi, D.; Sangregorio, C.; Sessoli, R.; Sorace, L. *J. Am. Chem. Soc.* **1999**, *121*, 5302–5310.
(22) Miyasaka, H.; Clerac, R.; Wernsdorfer, W.; Lecren, L.; Bonhomme, C.; Sugiura, K.; Yamashita, M. *Angew. Chem., Int. Ed.* **2004**, *43*, 2801–2805.
(23) Milios, C. J.; Vinslava, A.; Wernsdorfer, W.; Moggach, S.; Parsons, S.; Perlepes, S. P.; Christou, G.; Brechin, E. K. *J. Am. Chem. Soc.* **2007**, *129*, 2754–2755.

Published on Web 07/22/2010

interactions between Ln centers would generate remarkable magnetic behaviors as a result of their large intrinsic magnetic anisotropy. Indeed, the presence of large magnetic anisotropy in ferromagnetically coupled high-spin molecular systems may lead to the slow relaxation of the magnetization. Therefore, the synthesis and investigation of molecular magnetic materials based on lanthanide complexes represent a current challenging area of Inorganic Chemistry and Physical Chemistry. Actually, Ln-containing SMMs are increasingly reported in the literature,[24−26] most of them containing dysprosium(III) ions.[24,27−36]

A number of cubane clusters displaying SMM behavior have been described,[14,37−42] including dysprosium ones.[43] Recently, some of us have reported a Dy_4 cubane showing slow relaxation of magnetization.[44] On the basis of these interesting results, we have now prepared a new Dy cubane complex, that is, $[Dy_4(\mathbf{HL})_4(C_6H_4NH_2COO)_2(\mu_3\text{-}OH)_4(\mu\text{-}OH)_2(H_2O)_4]\cdot 4CH_3CN\cdot 12H_2O$ (**1**), and a bis-Dy cubane, that is, $Dy_8(\mathbf{HL})_{10}(C_6H_4NH_2COO)_2(\mu_3\text{-}OH)_8(OH)_2(NO_3)_2(H_2O)_4]$ (**2**), from a potentially tetradentate Schiff-base ligand, namely, 2-{[(2-hydroxy-3-methoxyphenyl)methylidene]amino}benzoic acid ($\mathbf{H_2L}$). The solid-state structures of **1** and **2** have been determined by single-crystal X-ray diffraction, and their magnetic properties have been thoroughly investigated. Compound **2** shows a SMM behavior while compound **1** does not display slow relaxation of magnetization. A closer look at the structural features of their $[Dy_4(\mu_3\text{-}OH)_4]$ cores reveals significant disparities of the respective cubane M−O−M angles (induced by two additional μ-OH^- bridges in **1**). These differences of the cubane metric parameters are most responsible for the distinct magnetic-exchange interactions observed.

Experimental Section

Materials and Methods. All starting materials were of A.R. Grade and used as received. The elemental analyses for C, H, and N were performed with a Perkin-Elmer 2400 analyzer. The IR measurements were recorded on a VERTEX 70 Fourier transform infrared (FTIR) spectrophotometer using the reflectance technique (4000−300 cm^{-1}); the samples were prepared as KBr disks. The Schiff base ligand $\mathbf{H_2L}$, that is, 2-{[(2-hydroxy-3-methoxyphenyl)methylidene]amino}benzoic acid, was obtained by condensation of anthranilic acid and *o*-vanillin in methanol, applying a previously reported synthetic method.[45]

Magnetic measurements were performed in the temperature range 1.9−300 K, using a Quantum Design MPMS-XL SQUID magnetometer equipped with a 7 T magnet. The diamagnetic corrections for the compounds were estimated using Pascal's constants,[46] and magnetic data were corrected for diamagnetic contributions of the sample holder.

Synthesis of the Dy_4 Cubane Cluster $[Dy_4(HL)_4(C_6H_4NH_2COO)_2(\mu_3\text{-}OH)_4(\mu\text{-}OH)_2(H_2O)_4]\cdot 4CH_3CN\cdot 12H_2O$ (1). An aqueous solution of potassium hydroxide (0.45 mL, 0.20 mmol) was added to a solution of the Schiff-base ligand (0.20 mmol, 56 mg) in 10 mL of acetonitrile. The resulting reaction mixture was stirred for 40 min. Then, solid dysprosium chloride hexahydrate (0.20 mmol, 75 mg) was added, and the ensuing red solution was stirred for 1 h. Finally, 5 mL of methanol were added, and the reaction mixture was filtered. The filtrate was left unperturbed to allow the slow evaporation of the solvent. Red single crystals, suitable for X-ray diffraction analysis, were obtained after 2 weeks. These crystals were collected by filtration, washed with cold methanol and acetonitrile, and dried in air. Yield: 25 mg (19.5%, based on the ligand). Elemental analysis (%) calcd for $C_{82}H_{110}Dy_4N_{10}O_{42}$: C, 38.50, H, 4.33, N, 5.48; found C, 38.65, H, 4.31, N, 5.75. IR (KBr, cm^{-1}): 3436 (w), 2841 (m), 1636 (w), 1611 (w), 1597 (w), 1567 (w), 1539 (w), 1492 (w), 1466 (w), 1440 (w), 1400 (w), 1291 (m), 1280 (m), 1263 (m), 1235 (w), 1181 (w), 1100 (m), 1069 (s), 1035 (s), 966(s), 922 (s), 858(s), 839 (s), 738 (w), 688 (m), 669 (m), 661(m), 634(m), 593(m), 538(m), 466(m), 435(m).

Synthesis of the Bis-Dy_4 Cubane Cluster $[Dy_8(HL)_{10}(C_6H_4NH_2COO)_2(\mu_3\text{-}OH)_8(OH)_2(NO_3)_2(H_2O)_4]$ (2). A methanolic solution of potassium hydroxide (0.35 mL, 0.15 mmol) was added to the Schiff-base ligand (0.15 mmol, 42 mg) dissolved in 6 mL of ethanol. The reaction mixture was stirred for 40 min. Next, solid dysprosium nitrate hexahydrate (0.15 mmol, 68 mg) was added to the above mixture, and the resulting red solution was stirred for 1 h. Six milliliters of dichloromethane were subsequently added, and the reaction mixture was filtered. The ensuing filtrate was left unperturbed to allow the slow evaporation of the solvent. Red single crystals, suitable for X-ray diffraction analysis, were obtained after 3 weeks. These crystals were collected by filtration, washed with cold ethanol, and dried in air. Yield: 22 mg (32%, based on the ligand). Elemental analysis (%) calcd for $C_{164}H_{150}Dy_8N_{14}O_{64}$: C, 42.44, H, 3.26, N, 4.23; found C, 42.60, H, 3.09, N, 4.28. IR (KBr, cm^{-1}): 3445 (m), 3058 (m), 2935 (m), 2839 (m), 1598 (w), 1568 (m), 1540 (w), 1494 (m), 1469 (m), 1445 (w), 1358 (w), 1292 (m), 1235 (w), 1181 (m), 1100 (s), 1069 (s), 1032 (s), 967 (s), 914 (s), 857 (s), 788 (s), 739 (m), 696 (m), 664 (m), 634 (m), 565 (s), 540 (s), 466 (s), 422 (s).

X-ray Crystallographic Analysis and Data Collection. Crystallographic data and refinement details are given in Table 1. Suitable

(24) Lin, P. H.; Burchell, T. J.; Ungur, L.; Chibotaru, L. F.; Wernsdorfer, W.; Murugesu, M. *Angew. Chem., Int. Ed.* **2009**, *48*, 9489–9492.
(25) Xu, J. X.; Ma, Y.; Liao, D. Z.; Xu, G. F.; Tang, J.; Wang, C.; Zhou, N.; Yan, S. P.; Cheng, P.; Li, L. C. *Inorg. Chem.* **2009**, *48*, 8890–8896.
(26) Chen, Z.; Zhao, B.; Cheng, P.; Zhao, X. Q.; Shi, W.; Song, Y. *Inorg. Chem.* **2009**, *48*, 3493–3495.
(27) Layfield, R. A.; McDouall, J. J. W.; Sulway, S. A.; Tuna, F.; Collison, D.; Winpenny, R. E. P. *Chem.—Eur. J.* **2010**, *16*, 4442–4446.
(28) Langley, S. K.; Moubaraki, B.; Forsyth, C. M.; Gass, I. A.; Murray, K. S. *Dalton Trans.* **2010**, *39*, 1705–1708.
(29) Xu, G. F.; Wang, Q. L.; Gamez, P.; Ma, Y.; Clerac, R.; Tang, J.; Yan, S. P.; Cheng, P.; Liao, D. Z. *Chem. Commun.* **2010**, *46*, 1506–1508.
(30) Wang, Y.; Li, X. L.; Wang, T. W.; Song, Y.; You, X. Z. *Inorg. Chem.* **2010**, *49*, 969–976.
(31) Hussain, B.; Savard, D.; Burchell, T. J.; Wernsdorfer, W.; Murugesu, M. *Chem. Commun.* **2009**, 1100–1102.
(32) Hewitt, I. J.; Lan, Y. H.; Anson, C. E.; Luzon, J.; Sessoli, R.; Powell, A. K. *Chem. Commun.* **2009**, 6765–6767.
(33) Lin, P. H.; Burchell, T. J.; Clerac, R.; Murugesu, M. *Angew. Chem., Int. Ed.* **2008**, *47*, 8848–8851.
(34) Gamer, M. T.; Lan, Y.; Roesky, P. W.; Powell, A. K.; Clerac, R. *Inorg. Chem.* **2008**, *47*, 6581–6583.
(35) Tang, J.; Hewitt, I.; Madhu, N. T.; Chastanet, G.; Wernsdorfer, W.; Anson, C. E.; Benelli, C.; Sessoli, R.; Powell, A. K. *Angew. Chem., Int. Ed.* **2006**, *45*, 1729–1733.
(36) Westin, L. G.; Kritikos, M.; Caneschi, A. *Chem. Commun.* **2003**, 1012–1013.
(37) Galloway, K. W.; Whyte, A. M.; Wernsdorfer, W.; Sanchez-Benitez, J.; Kamenev, K. V.; Parkin, A.; Peacock, R. D.; Murrie, M. *Inorg. Chem.* **2008**, *47*, 7438–7442.
(38) Isele, K.; Gigon, F.; Williams, A. F.; Bernardinelli, G.; Franz, P.; Decurtins, S. *Dalton Trans.* **2007**, 332–341.
(39) Venegas-Yazigi, D.; Cano, J.; Ruiz, E.; Alvarez, S. *Phys. B* **2006**, *384*, 123–125.
(40) Yang, E. C.; Wernsdorfer, W.; Zakharov, L. N.; Karaki, Y.; Yamaguchi, A.; Isidro, R. M.; Lu, G. D.; Wilson, S. A.; Rheingold, A. L.; Ishimoto, H.; Hendrickson, D. N. *Inorg. Chem.* **2006**, *45*, 529–546.
(41) Moragues-Canovas, M.; Helliwell, M.; Ricard, L.; Riviere, E.; Wernsdorfer, W.; Brechin, E.; Mallah, T. *Eur. J. Inorg. Chem.* **2004**, 2219–2222.
(42) Castro, S. L.; Sun, Z. M.; Grant, C. M.; Bollinger, J. C.; Hendrickson, D. N.; Christou, G. *J. Am. Chem. Soc.* **1998**, *120*, 2365–2375.
(43) Savard, D.; Lin, P. H.; Burchell, T. J.; Korobkov, I.; Wernsdorfer, W.; Clerac, R.; Murugesu, M. *Inorg. Chem.* **2009**, *48*, 11748–11754.
(44) Gao, Y. J.; Xu, G. F.; Zhao, L.; Tang, J.; Liu, Z. L. *Inorg. Chem.* **2009**, *48*, 11495–11497.
(45) Fan, Y. H.; Bi, C. F.; Li, J. Y. *J. Radioanal. Nucl. Chem.* **2002**, *254*, 641–644.
(46) Bain, G. A.; Berry, J. F. *J. Chem. Educ.* **2008**, *85*, 532–536.

Table 1. .Crystal Data and Structure Refinement for $[Dy_4(\mathbf{HL})_4(C_6H_4NH_2COO)_2(\mu_3\text{-}OH)_4(\mu\text{-}OH)_2(H_2O)_4]\cdot 4CH_3CN\cdot 12H_2O$ (**1**) and $[Dy_8(\mathbf{HL})_{10}(C_6H_4NH_2COO)_2(\mu_3\text{-}OH)_8(OH)_2(NO_3)_2(H_2O)_4]$ (**2**)

	1	**2**
empirical formula	$C_{82}H_{110}Dy_4N_{10}O_{42}$	$C_{164}H_{150}Dy_8N_{14}O_{64}$
F_w (g mol^{-1})	2557.80	4640.98
crystal system	orthorhombic	monoclinic
space group	*Fddd*	*C*2/*c*
crystal color	red	red
crystal size (mm^3)	$0.15\times0.17\times0.19$	$0.12\times0.15\times0.19$
temperature (K)	187(2)	187(2)
a (Å)	10.0802(4)	32.6847(17)
b (Å)	40.8842(15)	27.4910(14)
c (Å)	44.0852(16)	24.9658(13)
β (deg)	90	107.327(1)
V (Å^3)	18168.4(12)	21414.7(19)
ρ_{calcd} (Mg/m^3)	1.870	1.439
μ (mm^{-1})	3.354	2.830
F(000)	10176	9088
θ for data collection (deg)	1.36−26.07	0.99−25.10
collected reflections	28938	54806
independent reflections	4510	19027
R_{int}	0.0555	0.1678
$R\,[I > 2\sigma(I)]$	0.0337	0.0747
wR (all data)	0.1060	0.2826
goodness of fit on F^2	1.075	1.013
largest diff. peak and hole (e Å^3)	−1.106 and 1.382	−1.672 and 2.700

Scheme 1. Representation of the Ligand 2-{[(2-Hydroxy-3-methoxyphenyl)methylidene]amino}Benzoic Acid ($\mathbf{H_2L}$)

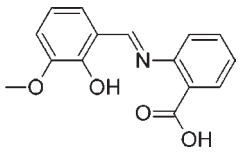

single crystals with dimensions of $0.19\times0.17\times0.15$ mm^3 and $0.19\times0.15\times0.12$ mm^3 for **1** and **2**, respectively, were selected for single-crystal X-ray diffraction analysis. Crystallographic data were collected at a temperature of 187(2) K on a Bruker ApexII CCD diffractometer with graphite monochromated Mo Kα radiation (λ = 0.71073 Å). Data processing was accomplished with the SAINT processing program.[47] The structure was solved by the direct methods and refined on F^2 by full-matrix least-squares using SHELXTL97.[48] The location of Dy atom was easily determined, and O, N, C, and H atoms were subsequently determined from the difference Fourier maps. The non-hydrogen atoms were refined anisotropically. The H atoms were introduced in calculated positions and refined with fixed geometry with respect to their carrier atoms. CCDC−778293 (**1**) and 778294 (**2**) contain the supplementary crystallographic data for this paper. These data can be obtained free of charge from the Cambridge Crystallographic Data Centre via www.ccdc.cam.ac.uk/data_request/cif.

Results and Discussion

The Schiff-base ligand 2-{[(2-hydroxy-3-methoxyphenyl)-methylidene]amino}benzoic acid ($\mathbf{H_2L}$) (Scheme 1) was obtained by simple condensation reaction between *o*-vanillin (2-hydroxy-3-methoxybenzaldehyde) and anthranilic acid (2-aminobenzoic acid) in methanol, following an earlier reported procedure.[45] The reactions of different dysprosium(III) salts (chloride or nitrate) with the ligand $\mathbf{H_2L}$ using several solvent combinations generate compounds with distinct structures. The formation mechanism for these different architectures is not clear as yet. However, the two additional μ-OH groups linking the Dy ions within the Dy_4 cubane, formed in the presence of water, instead of a bridging **HL** ligand and a terminal bidentate η^2-nitrate may prevent the formation of the $[Dy_4]_2$ structure (**2**), therefore resulting in the isolation of a discrete Dy_4 cubane (**1**).

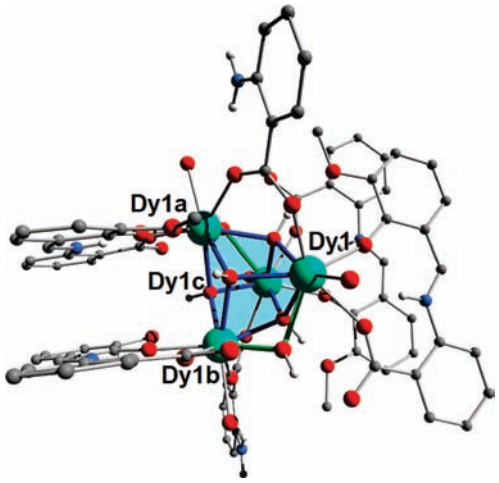

Figure 1. Representation of the molecular structure of $[Dy_4(\mathbf{HL})_4(C_6H_4NH_2COO)_2(\mu_3\text{-}OH)_4(\mu\text{-}OH)_2(H_2O)_4]\cdot 4CH_3CN\cdot 12H_2O$ (**1**), illustrating the Dy_4 cubane core. Only the H atoms involved in hydrogen-bonding interactions and from the μ_3- and μ-hydroxido ligands are shown for clarity. The blue bonds symbolize the μ_3-hydroxido ligands and the green bonds represent μ-hydroxido ligands. Symmetry operations: a = 5/4−*x*, 1/4−*y*, *z*; b = *x*, 1/4−*y*, 1/4−*z*; c = 5/4−*x*, *y*, 1/4−*z*.

Crystal Structure of $[Dy_4(HL)_4(C_6H_4NH_2COO)_2(\mu_3\text{-}OH)_4(\mu\text{-}OH)_2(H_2O)_4]\cdot 4CH_3CN\cdot 12H_2O$ (1). The reaction of $DyCl_3\cdot 6H_2O$ with a basic solution of $\mathbf{H_2L}$ in water/acetonitrile/methanol (see Experimental Section) produces red crystals of **1** after 2 weeks. Single-crystal X-ray studies revealed that **1** crystallizes in the orthorhombic space group *Fddd*. A perspective view of the molecular structure of **1** is represented in Figure 1. Details for the structure solution and refinement are summarized in Table 1, and selected bond distances and angles are listed in Table 2. The molecule is a tetranuclear dysprosium(III) cubane compound consisting of eight-coordinated metallic centers in a square antiprismatic coordination environment (Figure 2 and Supporting Information, Figure S1). The two square bases of the square antiprism are formed by the atoms (O1, O3, O6, and O6c) and (O5, O6a, O7, O8), respectively (Supporting Information, Figure S1). The Dy1 ion is coordinated by two carboxylato oxygen atoms (O1 and O5) belonging respectively to one $\mathbf{HL}^-$ ligand and one anthranilato moiety (resulting from the hydrolysis of a $\mathbf{H_2L}$ molecule), a phenolato oxygen atom (O3), three μ_3-OH^- groups (oxygen atoms O6, O6a, and O6c), a μ-OH^- ligand (oxygen atom O7), and a water molecule (oxygen atom O8; Figure 2B). The Dy−O_{COO}, Dy−O_{PhO}, Dy−O_{OH}, and Dy−O_{H2O} bond distances can be considered as normal (Table 2).[49−51] A square antiprism can be described by an angle describing its elongation or flatness.[52] This parameter, that is, α, is the angle between the

(47) *SAINT*, 7.36a; Bruker AXS: Madison, WI.
(48) Sheldrick, G. M. *Acta Crystallogr., Sect. A* **2008**, *64*, 112–122.
(49) Gerasko, O. A.; Mainicheva, E. A.; Naumova, M. I.; Neumaier, M.; Kappes, M. M.; Lebedkin, S.; Fenske, D.; Fedin, V. P. *Inorg. Chem.* **2008**, *47*, 8869–8880.
(50) Shi, Q. S.; Zhang, S.; Wang, Q.; Ma, H. W.; Yang, G. Q.; Sun, W. H. *J. Mol. Struct.* **2007**, *837*, 185–189.
(51) Brzyska, W.; Rzaczynska, Z.; Swita, E.; Mrozek, R.; Glowiak, T. *J. Coord. Chem.* **1997**, *41*, 1–12.
(52) Adam, S.; Ellern, A.; Seppelt, K. *Chem.—Eur. J.* **1996**, *2*, 398–402.

Table 2. Selected Bond Distances (Angstroms) and Angles (Degrees) for $[Dy_4(\mathbf{HL})_4(C_6H_4NH_2COO)_2(\mu_3\text{-}OH)_4(\mu\text{-}OH)_2(H_2O)_4]\cdot 4CH_3CN\cdot 12H_2O$ (**1**)[a]

Dy1			
Bond Distances (Å)			
Dy1−O1	2.369(4)	Dy1−O3	2.279(4)
Dy1−O5	2.333(4)	Dy1−O6	2.345(4)
Dy1−O7	2.521(4)	Dy1−O8	2.421(4)
Dy1−O6a	2.372(4)	Dy1−O6c	2.348(4)
Bond Angles (deg.)			
O1−Dy1−O3	69.55(14)	O3−Dy1−O6	81.02(14)
O6−Dy1−O6c	69.16(13)	O6c−Dy1−O1	75.12(13)
O5−Dy1−O6a	76.58(14)	O6a−Dy1−O7	67.72(11)
O7−Dy1−O8	73.39(12)	O8−Dy1−O5	71.56(14)
O1−Dy1−O6 (γ angle)[b]	127.09(13)	O3−Dy1−O6c (γ angle)	101.96(14)
α angle (O1, O6)[c]	63.55(13)	α angle (O3, O6c)	50.98(14)
O5−Dy1−O7 (γ angle)	117.45(11)	O6a−Dy1−O8 (γ angle)	108.35(14)
α angle (O5, O7)	58.73(11)	α angle (O6a, O8)	54.18

[a] Symmetry operations: a, 5/4−x, 1/4−y, z; c, 5/4−x, y, 1/4−z. [b,c] See Figure 3 for the definitions of the angles α and γ.

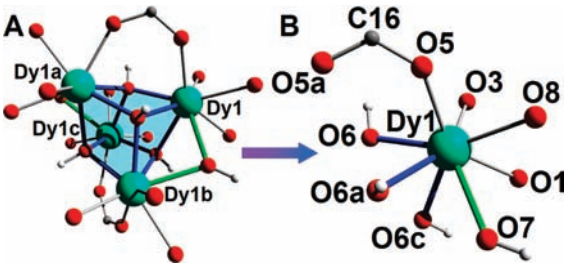

Figure 2. (A) Representation of the Dy_4 cubane core and (B) coordination environment of the dysprosium(III) ion. Only the hydrogen atoms from the μ_3-OH^- groups are shown for clarity. The blue bonds symbolize the μ_3-hydroxido ligands and the green bonds represent μ-hydroxido ligands. Symmetry operations: a = 5/4−x, 1/4−y, z; b = x, 1/4−y, 1/4−z; c = 5/4−x, y, 1/4−z.

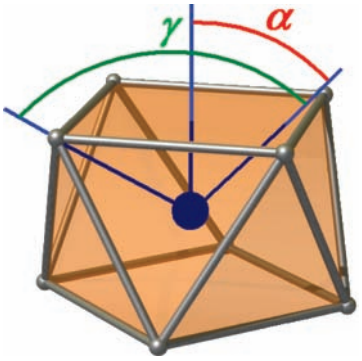

Figure 3. Definition of the angle α in a regular square antiprism.[53] γ is the angle between opposite ligands within one hemisphere; α = γ/2.[52]

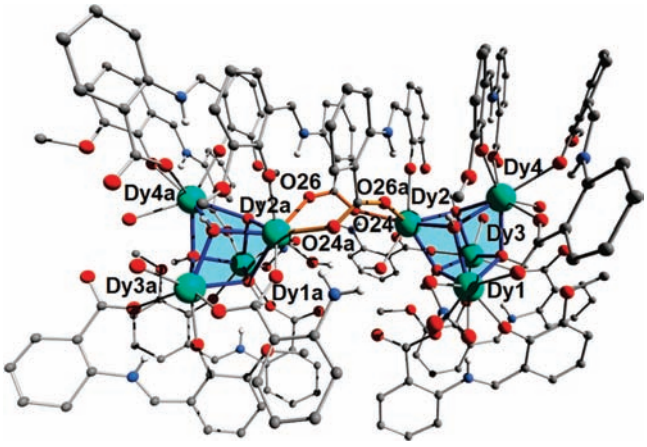

Figure 4. Representation of the molecular structure of octanuclear $[Dy_8(\mathbf{HL})_{10}(C_6H_4NH_2COO)_2(\mu_3\text{-}OH)_8(OH)_2(NO_3)_2(H_2O)_4]$ (**2**), showing the two cubane units doubly bridged by μ-O,O'-carboxylato ligands (oxygen atoms O26, O26a, O24, and O24a; orange bonds). The blue bonds symbolize the μ_3-hydroxido ligands. Only the H atoms involved in hydrogen-bonding interactions and from the μ_3- and μ-hydroxido ligands are shown for clarity. Symmetry operation: a = −x, y, 1/2−z.

S_8 axis of the square antiprism and the central atom ligand bond (Figure 3).[53,54] This angle is also defined as α = γ/2, γ being the angle between opposite bonds within one hemisphere (Figure 3). For a soft-sphere model with a repulsion energy law ≈1/ r^6, the ideal α value amounts to 57.16°.[53,54] For **1**, the α angles vary from 50.98(14) to 63.55(13)° (Table 2). Actually, the hemisphere including the atoms (O1, O3, O6, and O6c) is strongly distorted, since the angles $\alpha_{(O1,O6)}$ = 63.55(13)° and $\alpha_{(O6,O6c)}$ = 50.98(14)° are respectively 6.39° and 6.18° outside the perfect value. This distortion is most likely due to both the very small bite angle of the ligand $\mathbf{HL}^-$ (O1−Dy−O3 = 69.55(14)°), and the coordination of two μ_3-OH^- ligands (O6−Dy1−O6c = 69.16(13)°). The second hemisphere is characterized by α angles of 58.73(11) and 54.18° (Table 2), closer to the expected value for a regular square antiprism. Thus, the self-assembly between four symmetry-related Dy^{III} ions, four μ_3-hydroxido ligands, four $\mathbf{HL}^-$ ligands, four water molecules, two anthranilato groups and two μ_2-hydroxido ligands generates a distorted cubane core (Figure 2A). Within this tetranuclear cluster, each Dy^{III} ion is connected to three neighbors through μ_3-OH^- ligands (see blue bonds in Figure 2A). In addition, the metal centers Dy1 and Dy1b, and Dy1a and Dy1c are bridged by μ-hydroxido units (see green bonds in Figure 2A). Finally, the metals Dy1 and Dy1a, and Dy1b and Dy1c are connected by μ-O,O'-carboxylato ligands (respectively, O5 and O5a and O5b and O5c). The resulting cubic array of alternating dysprosium and oxygen atoms exhibits intracluster metal···metal separation distances in the range 3.589(1)−3.832(1) Å. The crystal packing of **1** reveals the formation of one-dimensional (1-D) supramolecular chains along the crystallographic a axis (Supporting Information, Figure S2). The 1-D chain is assembled through π−π stacking interactions between the anthranilic groups of $\mathbf{HL}^-$ ligands belonging to adjacent Dy_4 units (centroid-to-centroid distance of 3.474(4) Å). The shortest intercubane Dy···Dy distance, namely, 7.643(1) Å, is found in this self-organized chain (Supporting Information, Figure S2A).

The crystal structure of **1** exhibits intramolecular hydrogen bonds involving the imino (N1) and the amino (N2) N−H moieties of the $\mathbf{HL}^-$ and anthranilato ligands, respectively (Supporting Information, Table S1). In addition, an intricate network of intra- and intermolecular O−H···O bonds is observed (Supporting Information, Table S1).

(53) Kepert, D. L. *Stereochemistry in Inorganic Chemistry Concepts*; Springer: Berlin, Germany, 1982; Vol. *6*.
(54) Kepert, D. L. *Prog. Inorg. Chem.* **1978**, *24*, 179–249.

Table 3. Selected Bond Distances (Angstroms) and Angles (Degrees) for $[Dy_8(\mathbf{HL})_{10}(C_6H_4NH_2COO)_2(\mu_3\text{-}OH)_8(OH)_2(NO_3)_2(H_2O)_4]$ (**2**)[a]

Dy1			
Bond Distances (Å)			
Dy1−O2	2.313(11)	Dy1−O3	2.254(11)
Dy1−O5	2.361(12)	Dy1−O21	2.463(13)
Dy1−O22	2.585(14)	Dy1−O28	2.351(10)
Dy1−O29	2.330(8)	Dy1−O31	2.342(11)
Bond Angles (deg.)			
O3−Dy1−O22	84.2(4)	O22−Dy1−O21	50.6(4)
O21−Dy1−O29	74.4(4)	O29−Dy1−O28	71.3(3)
O28−Dy1−O3	76.9(4)	O2−Dy1−O5	134.0(4)
O5−Dy1−O31	149.7(4)	O2−Dy1−O31	76.1(4)
Dy2			
Bond Distances (Å)			
Dy2−O9	2.317(11)	Dy2−O16	2.302(11)
Dy2−O24	2.454(10)	Dy2−O26a	2.355(11)
Dy2−O27	2.383(10)	Dy2−O29	2.376(10)
Dy2−O30	2.369(10)	Dy2−O31	2.382(11)
Bond Angles (deg.)			
O16−Dy2−O24	70.5(4)	O24−Dy2−O27	80.1(3)
O27−Dy2−O31	71.1(4)	O31−Dy2−O16	75.9(4)
O9−Dy2−O26a	71.0(4)	O26a−Dy2−O29	73.3(4)
O29−Dy2−O30	69.5(3)	O30−Dy2−O9	76.0(4)
O16−Dy2−O27 (γ angle)[b]	97.0(4)	O24−Dy2−O31 (γ angle)	132.2(4)
α angle (O16, O27)[c]	48.5(4)	α angle (O24, O31)	66.1(4)
O9−Dy2−O29 (γ angle)	91.3(4)	O26a−Dy2−O30 (γ angle)	128.9(4)
α angle (O9, O29)	45.7(4)	α angle (O26a, O30)	64.5(4)
Dy3			
Bond Distances (Å)			
Dy3−O12	2.318(14)	Dy3−O13	2.276(11)
Dy3−O15	2.289(13)	Dy3−O25	2.405(11)
Dy3−O28	2.334(10)	Dy3−O30	2.318(11)
Dy3−O31	2.330(11)		
Bond Angles (deg.)			
O12−Dy3−O13	72.6(4)	O13−Dy3−O28	107.4(4)
O28−Dy3−O12	82.1(4)	O15−Dy3−O25	79.4(4)
O25−Dy3−O30	75.8(4)	O30−Dy3−O15	86.9(4)
O31−Dy3−O13	83.6(4)	O31−Dy3−O15	84.0(4)
O31−Dy3−O30	71.5(4)	O31−Dy3−O28	70.4(4)
Dy4			
Bond Distances (Å)			
Dy4−O6	2.317(13)	Dy4−O7	2.418(12)
Dy4−O18	2.339(11)	Dy4−O19	2.281(11)
Dy4−O28	2.377(8)	Dy4−O29	2.408(10)
Dy4−O30	2.357(10)	Dy4−O32	2.411(13)
Bond Angles (deg.)			
O7−Dy4−O6	66.3(4)	O6−Dy4−O28	75.6(4)
O28−Dy4−O32	73.3(4)	O32−Dy4−O7	69.7(4)
O18−Dy4−O19	73.4(4)	O19−Dy4−O29	80.6(4)
O29−Dy4−O30	69.2(3)	O30−Dy4−O18	73.8(4)
O6−Dy4−O32 (γ angle)[b]	97.8(4)	O7−Dy4−O28 (γ angle)	121.2(4)
α angle (O6, O32)[a]	48.9(4)	α angle (O7, O28)	60.6(4)
O18−Dy4−O29 (γ angle)	126.7(4)	O19−Dy4−O30 (γ angle)	104.8(4)
α angle (O18, O29)	63.4(4)	α angle (O19, O30)	52.4(4)

[a] Symmetry operations: a, $-x$, y, $1/2-z$. [b,c] See Figure 3 for the definitions of the angles α and γ.

Crystal Structure of $[Dy_8(HL)_{10}(C_6H_4NH_2COO)_2(\mu_3\text{-}OH)_8(OH)_2(NO_3)_2(H_2O)_4]$ (2). The reaction of $Dy(NO_3)_3\cdot 6H_2O$ with a basic solution of $\mathbf{H_2L}$ in methanol/ethanol/dichloromethane (see Experimental Section) yields red crystals of **2** after three weeks. The single-crystal X-ray structure of the octanuclear compound is depicted in Figure 4. Compound **2** crystallizes in the monoclinic space group $C2/c$. Details for the structure solution and refinement are summarized in Table 1, and selected bond distances and angles are listed in Table 3. **2** consists of two symmetry-related $[Dy_4(\mu_3\text{-}OH)_4]$ cubanes doubly bridged by μ-O,O'-carboxylato groups (oxygen atoms O26, O26a, O24 and O24a; orange bonds in Figure 4), belonging to two shared $\mathbf{HL}^-$ ligands. The tetranuclear core contains four different dysprosium(III) ions (Figures 4 and 5).

The metal center Dy1 is eight-coordinated by one bidentate $\mathbf{HL}^-$ ligand (through the phenolato oxygen atom O3 and the oxygen atom O2 from a monodentate carboxylato group), a carboxylato oxygen atom (O5) from a bridging $\mathbf{HL}^-$ ligand, a bidentate nitrate anion (O21 and O22), and three μ_3-hydroxido ligands (O28, O29, and O31; Figure 5B). The coordination geometry of Dy1 is best described as a hula hoop-like geometry (Supporting Information, Figure S3), by analogy with the environment described in the literature for the nine-coordinate compound $[La_2I_2(OH)_2(\text{dibenzo-18-crown-6})_2]I(I_3)$.[55,56] In **2**, the cyclic ring (hula hoop) is defined by the atoms O3, O22, O21, O29, and O28 (Supporting Information, Figure S3). The Dy−O_{COO}, Dy−O_{PhO}, Dy−O_{OH}, and Dy−O_{NO3} bond lengths are in normal ranges (Table 3).[31,57]

The eight-coordinated Dy2 ion exhibits a square-antiprismatic coordination environment formed by one bidentate $\mathbf{HL}^-$ ligand (O9 and O26a), whose μ-O,O'-carboxylato group acts as a bridge between the two cubanes, a carboxylato oxygen atom (O24) from a second $\mathbf{HL}^-$ ligand coordinated to the adjacent cubane unit, a carboxylato oxygen atom (O16) belonging to an intracubane bridging anthranilato ligand, one monodentate hydroxido (O27) ligand, and three μ_3-hydroxido ligands (O29, O30, and O31; Figure 5C). The Dy−O_{COO}, Dy−O_{PhO}, and Dy−O_{OH} bond distances are comparable to those reported for Dy^{III} clusters (Table 3).[31,58] The angles α, defining the regularity of a square antiprism,[54] for Dy2 range from 45.7(4) to 66.1(4)° (Table 3). The first hemisphere containing the atoms (O16, O24, O27, and O31; Supporting Information, Figure S4) is strongly distorted, as reflected by the angles $\alpha_{(O16,O27)}$ and $\alpha_{(O24,O31)}$ of 48.5(4) and 66.1(4)°, respectively (the ideal α value is 57.16°). The distortion is mainly caused by steric constraints arising from the bridging of Dy2 to the other three metal centers of the cubane, through three μ_3-OH^- anions and a μ-O,O'-anthranilato group (see Figure 5A), and from the involvement of Dy2 in the formation of the biscubane unit, via two μ-O,O'-carboxylato bridges connecting Dy2 to Dy2a (see orange bonds in Figure 4). The second hemisphere (O9, O26a, O29, and O30; Supporting

(55) Ruiz-Martinez, A.; Casanova, D.; Alvarez, S. *Chem.—Eur. J.* **2008**, *14*, 1291–1303.
(56) Runschke, C.; Meyer, G. *Z. Anorg. Allg. Chem.* **1997**, *623*, 1493–1495.
(57) Gu, X. J.; Xue, D. F. *Inorg. Chem.* **2007**, *46*, 3212–3216.
(58) Zhang, M. B.; Zhang, J.; Zheng, S. T.; Yang, G. Y. *Angew. Chem., Int. Ed.* **2005**, *44*, 1385–1388.

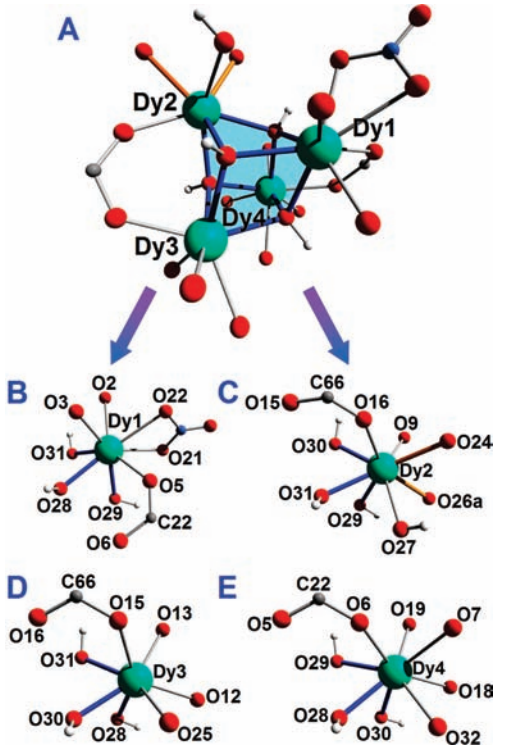

Figure 5. (A) Cubane core of compound **2**; (B) coordination environment of the dysprosium(III) ion Dy1, (C) Dy2, (D) Dy3, and (E) Dy4. Only the hydrogen atoms from the μ_3-OH^- and OH^- groups are shown for clarity. The blue bonds symbolize the μ_3-hydroxido ligands and the orange bonds represent the bridging μ-*O*,*O*′-carboxylato ligands. Symmetry operation: a = $-x$, y, $1/2-z$.

Information, Figure S4) of the square antiprism is strongly distorted as well, the α angles being $\alpha_{(O9,O29)}$ = 45.7(4)° and $\alpha_{(O26a,O30)}$ = 64.5(4)° (Table 3). Again, this distortion most likely arises from the creation of the bis-cubane structure which clearly generates steric constraints.

The seven-coordinated Dy3 ion adopts a capped trigonal-prismatic geometry (Supporting Information, Figures S5 and 5D. The trigonal prism is formed by one bidentate $\mathbf{HL}^-$ ligand (O12 and O13), one oxygen atom (O15) from a bridging anthranilato ligand, two μ_3-OH^- groups (O28 and O30), and one water molecule (O25). The capped ligand is a μ_3-OH^- anion (O31) connecting Dy3 to Dy1 and Dy2. The regularity of a trigonal prism is defined by the torsion angles α involving opposite corners and the centroids of the trigonal faces (Figure 6).[59] For a regular trigonal prism, these angles α are equal to 0°. For Dy3, the angles α amount to 6.18, 11.20 and 14.17°. These significant deviations from the ideal value of 0° are because the trigonal faces (O15, O25, O30) and (O12, O13, O28) are not perfectly equilateral (Supporting Information, Figure S5B). In addition, these two faces are not parallel, as illustrated by a dihedral angle between them of 4.38°. This distortion may be ascribed to the small bite angle of the $\mathbf{HL}^-$ ligand (O12−Dy3−O13 = 72.6(4)°), and to the coordination of three μ_3-hydroxido ligands to Dy3 generating the $[Dy_4(\mu_3\text{-}OH)_4]$ core. The Dy−O_{COO}, Dy−O_{PhO}, and Dy−O_{OH} bond lengths are in normal ranges (Table 3).[58,60]

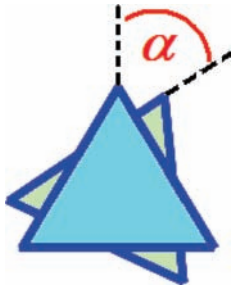

Figure 6. Angle α characterizing the distortion of a trigonal prism.[59].

As depicted in Figures 4 and 5E, Dy4 is eight-coordinated by two π-stacked $\mathbf{HL}^-$ ligands, three μ_3-OH^- groups (O28, O29 and O30), and one water molecule (O32). The coordination geometry of Dy4 is best described as a distorted square antiprism (Supporting Information, Figure S6). The angles α, defining the regularity of a square antiprism,[54] for Dy4 range from 48.9(4) to 63.4(4)° (Table 3) and therefore significantly outside the standard value of 57.16°. Thus, the first hemisphere containing the atoms (O6, O7, O32, and O28; Supporting Information, Figure S6) is characterized by the values $\alpha_{(O6,O32)}$ = 48.9(4)° and $\alpha_{(O7,O28)}$ = 60.6(4)° (Table 3). The second distorted hemisphere (O18, O19, O29, O30) is defined by the α angles $\alpha_{(O18,O29)}$ = 63.4(4)° and $\alpha_{(O19,O30)}$ = 52.4(4)° (Table 3). The distortion of the square antiprism may be explained by both the small bite angle of the $\mathbf{HL}^-$ ligand (O6−Dy4−O7 = 66.3(4)°), and the steric constraints induced by the formation of the cubane core. The Dy−O_{COO}, Dy−O_{PhO}, and Dy−O_{OH} bond distances can be considered as typical for such DyO_8 coordination environments.[57,58]

The self-assembly between the four different Dy^{III} ions, five $\mathbf{HL}^-$ ligands, four μ_3-hydroxido ligands, one OH^- and one NO_3^- anions, and two water molecules produces a cubic $[Dy_4(\mathbf{HL})_5(C_6H_4NH_2COO)(\mu_3\text{-}OH)_4(OH)(NO_3)(H_2O)_2]$ cluster. Within this tetranuclear cluster, each Dy^{III} ion is connected to the other three metal centers via three μ_3-OH^- bridges. In addition, Dy1 and Dy4 are linked by the μ-*O*,*O*′-carboxylato group of a $\mathbf{HL}^-$ ligand (oxygen atoms O5 and O6), and Dy2 and Dy3 are bridged by a μ-*O*,*O*′-anthranilato ligand (oxygen atoms O15 and O16). In the resulting $[Dy_4(\mu_3\text{-}OH)_4]$ cubane, the intramolecular Dy···Dy separation distances are in the range 3.674(1)− 3.853(1) Å. This cubane is connected to an adjacent symmetry-related cubane by two μ-*O*,*O*′-carboxylato units (see orange bonds in Figure 4), belonging to two $\mathbf{HL}^-$ ligands (whose phenolato parts are coordinated to distinct cubanes), thus generating the octanuclear compound **2**. The shortest intramolecular, intercubane metal···metal distance is Dy2···Dy2a = 5.889(1) Å. The crystal packing of **2** reveals the formation of a supramolcular 1-D zigzag chain along the crystallographic *c* axis, through the association of Dy_8 clusters by means of π−π interactions between $\mathbf{HL}^-$ ligands (centroid-to-centroid distance of 3.607(11); Supporting Information, Figure S7). This crystal-packing arrangement is of a scalelike network observed in a manganese(II)-azido framework.[61] The shortest Dy···Dy within the zigzag chains is 8.737(1) Å. The arrangement of these 1-D chains in the crystal lattice

(59) Sreerama, S. G.; Pal, S.; Pal, S. *Inorg. Chem. Commun.* **2001**, *4*, 656–660.
(60) Xu, N.; Shi, W.; Liao, D. Z.; Yan, S. P. *Inorg. Chem. Commun.* **2007**, *10*, 1218–1221.
(61) Gao, E. Q.; Bai, S. Q.; Wang, Z. M.; Yan, C. H. *J. Am. Chem. Soc.* **2003**, *125*, 4984–4985.

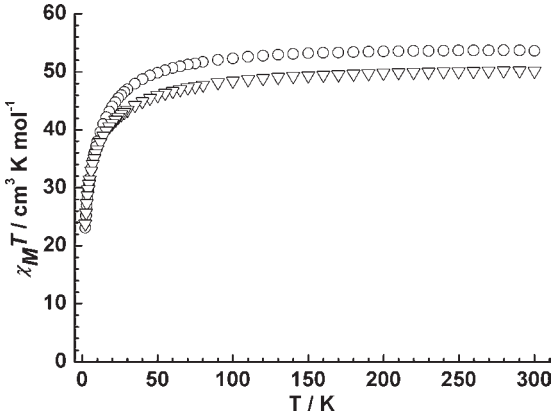

Figure 7. Temperature dependence of the $\chi_M T$ products at 1 kOe for **1** (open cycle) and **2** (open triangle), normalizing all the data per Dy_4 unit.

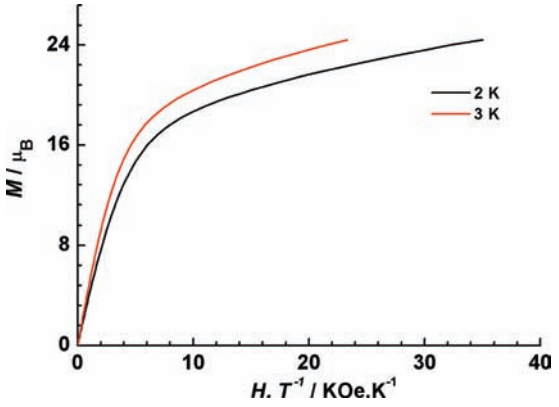

Figure 8. M versus H/T plots for **1** at 2 and 3 K.

produces infinite channels (Supporting Information, Figure S8). The shortest interchain Dy···Dy separation distance is 8.733(1) Å.

The crystal structure of **2** exhibits an intricate network of intramolecular N−H···O and O−H···O hydrogen bonds (Supporting Information, Table S2). In addition, the Dy8 clusters are interconnected through O−H···O bonds (Supporting Information, Table S2).

Magnetic Properties. Direct-current (dc) magnetic susceptibility studies of **1** and **2** have been carried out in an applied magnetic field of 1000 Oe in the temperature range 300−2 K. The plot of $\chi_M T$ versus T, where χ_M is the molar magnetic susceptibility, is shown in Figure 7. The observed $\chi_M T$ value at 300 K of 53.6 cm^3 K mol^{-1} for **1** (50.2 cm^3 K mol^{-1} for **2**) is lower than the expected value of 56.7 cm^3 K mol^{-1} for four uncoupled Dy^{III} ions (S = 5/2, L = 5, $^6H_{15/2}$, g = 4/3). $\chi_M T$ gradually decreases until 50 K and then further decreases to reach a minimum of 23.1 cm^3 K mol^{-1} for **1** (23.8 cm^3 K mol^{-1} for **2**) at 2 K, indicating a progressive depopulation of excited Stark sublevels.

Magnetization (M) data for **1** and **2** were collected in the 0−70 kOe field range below 5 K. The non-superimposition of the M versus H/T data on a single master-curve (Figures 8 and 9) suggests the presence of a significant magnetic anisotropy and/or low-lying excited states. The magnetization eventually reaches the value of 24.4 μ_B for **1** (22.2 μ_B for **2**) at 2 K and 70 kOe without clear saturation. This value is much lower than the expected

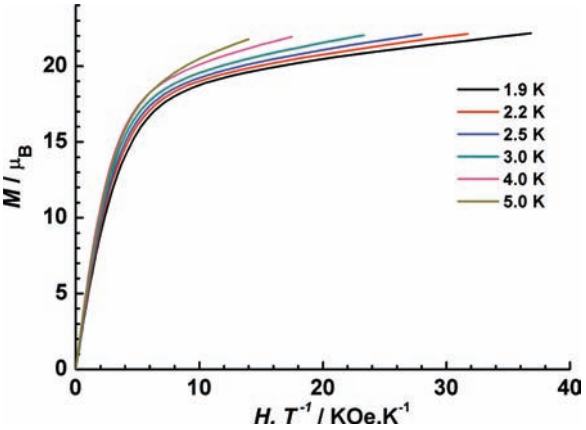

Figure 9. M versus H/T plots for **2** at different temperatures below 5 K, by normalizing the data per Dy_4 unit.

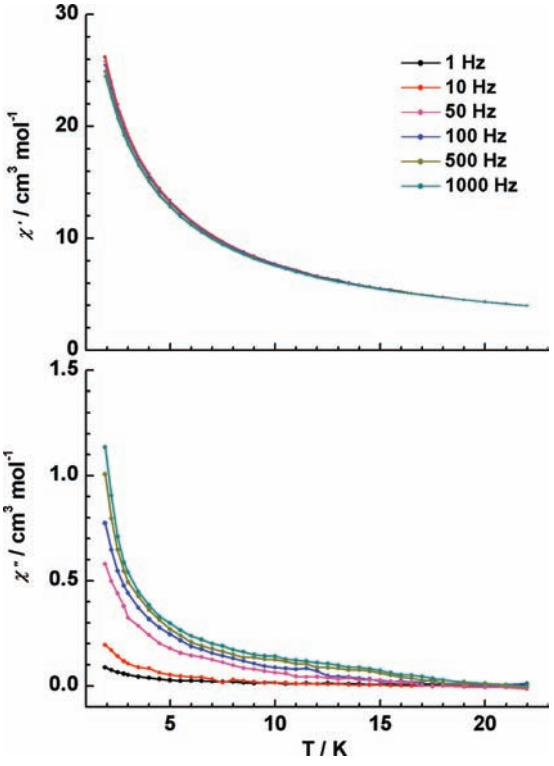

Figure 10. Temperature dependence of the in-phase (top) and out-of-phase (bottom) ac susceptibility for **2** under zero dc field.

saturation value of 40 μ_B for four non-interacting Dy^{III} ions, most likely due to the crystal-field effect at the Dy^{III} ion that eliminates the 16-fold degeneracy of the $^6H_{15/2}$ ground state.[35]

Alternating current (ac) susceptibility measurements were carried out for **1** and **2** under a zero-dc field to investigate the dynamics of the magnetization. As shown in the Supporting Information, Figure S9, **1** does not exhibit any out-of-phase ac signal. The dynamics of magnetization for **2** were also investigated from ac susceptibility measurements, in a zero-static field and in a 3.0 Oe ac field oscillating at the indicated frequencies given in Figure 10 (as the plots of χ' vs T and χ'' vs T). Strikingly, a frequency-dependent increase of the in-phase signal together with the concomitant appearance of an out-of-phase signal is observed, indicating the onset of slow magnetization

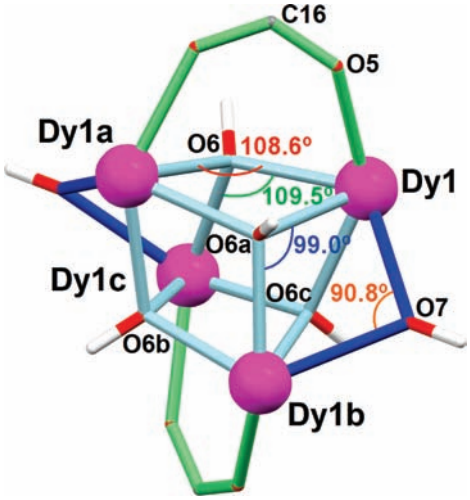

Figure 11. Cubane core of compound **1** showing characteristic M−O−M angles involving μ-hydroxido and μ_3-hydroxido bridging ligands.

relaxation. Although such ac signals are observed above 1.9 K, no hysteresis is noticed in the graph of *M* versus. *H* (Supporting Information, Figure S10), obtained using a traditional SQUID magnetometer. The non-occurrence of a hysteresis may be caused by the presence of a relatively fast zero-field relaxation.

Structure−Property Relationship. The cubane cores in compounds **1** and **2** are a priori comparable (see Figures 2A and 5A). However, the magnetic properties are drastically different (see section above). Indeed, the Dy_4 compound **1** does not exhibit any out-of-phase ac signal, while the bis-Dy_4 compound **2** shows a slow magnetic relaxation of magnetization. These distinct magnetic behaviors must be caused by subtle but crucial structural differences between the respective $[Dy_4(\mu_3\text{-}OH)_4]$ cores. Actually, a closer look at the two cubic arrangements reveals important disparities.

As is evidenced in Figure 11, each Dy^{III} ion in **1** is linked to the three other metal centers via μ_3-OH^- bridges (light-blue bonds in Figure 11). In addition, Dy1 is diagonally bridged to Dy1b through a μ-OH^- ligand; Dy1a and Dy1c are connected in the same way (see dark-blue bonds in Figure 11). The resulting cubane is defined by Dy−O bonds varying from 2.345(4) to 2.372(4) Å (Table 2). The Dy−O−Dy cubane angles range from 99.00(14) to 109.50(15)° (Table 4). The four small angles Dy1−O6a−Dy1b, Dy1−O6c−Dy1b, Dy1a−O6−Dy1c, and Dy1a−O6b−Dy1c of 99.00(14)° (compare to the eight other Dy−O−Dy angles which are above 108°) obviously results from the μ-OH^--bridging of Dy1 to Dy1b, and of Dy1a to Dy1c (angle Dy1−O7−Dy1b = 90.75(16)°; Table 4). The metal···metal distances are in the range 3.589(1)−3.832(1) Å (Table 4).

In compound **2** (Figure 12), the cubane Dy−O bonds vary from 2.318(11) to 2.408(11) Å (Table 3). The Dy−O−Dy angles of the cubane lie between 102.5(4) and 109.3(4)° (Table 4). Thus, in contrast to **1**, all angles in **2** are well above 99°. The metal···metal distances range from 3.674(1) to 3.853(1) Å (Table 4).

The main, significant disparities between the two cubic arrays are thus found in the Dy−O−Dy angles. Therefore, the distinct magnetic properties observed for compounds **1** and **2** are most likely due to different magnetic

Table 4. Selected Important Bond Distances (Angstroms) and Angles (Degrees) for the Cubane Cores in Compounds **1**, **2** and $[Dy_4(\mu_3\text{-}OH)_4(isonicotinate)_6(py)(CH_3OH)_7](ClO_4)_2\cdot py\cdot 4CH_3OH$ (**3**)[44]

Compound **1**[a]			
Bond Distances (Å)			
Dy1−Dy1a	3.831(1)	Dy1−Dy1b	3.589(1)
Dy1−Dy1c	3.832(1)		
Bond Angles (deg.)			
Dy1−O6−Dy1a	108.60(15)	Dy1−O6a−Dy1b	99.00(14)
Dy1−O6−Dy1c	109.50(15)	Dy1−O7−Dy1b	90.75(16)

Compound **2**			
Bond Distances (Å)			
Dy1−Dy2	3.729(1)	Dy1−Dy3	3.785(2)
Dy1−Dy4	3.805(1)	Dy2−Dy3	3.768(1)
Dy2−Dy4	3.853(1)	Dy3−Dy4	3.674(1)
Bond Angles (deg.)			
Dy1−O28−Dy4	107.2(4)	Dy1−O29−Dy4	106.8(4)
Dy1−O29−Dy2	104.8(3)	Dy1−O31−Dy2	104.2(4)
Dy1−O28−Dy3	107.8(4)	Dy1−O31−Dy3	108.2(5)
Dy2−O30−Dy3	107.0(4)	Dy2−O31−Dy3	106.2(4)
Dy2−O29−Dy4	107.3(4)	Dy2−O30−Dy4	109.3(4)
Dy3−O28−Dy4	102.5(4)	Dy3−O30−Dy4	103.6(4)

$[Dy_4(\mu_3\text{-}OH)_4(isonicotinate)_6(py)(CH_3OH)_7](ClO_4)_2\cdot py\cdot 4CH_3OH$[44]			
Bond Distances (Å)			
Dy1−Dy2	3.783(1)	Dy1−Dy3	3.725(1)
Dy1−Dy4	3.761(1)	Dy2−Dy3	3.720(1)
Dy2−Dy4	3.811(1)	Dy3−Dy4	3.857(1)
Bond Angles (deg.)			
Dy1−O13−Dy4	106.22(16)	Dy1−O14−Dy4	105.19(16)
Dy1−O13−Dy2	103.99(16)	Dy1−O15−Dy2	108.36(17)
Dy1−O14−Dy3	104.40(15)	Dy1−O15−Dy3	105.52(16)
Dy2−O15−Dy3	105.25(16)	Dy2−O16−Dy3	103.65(16)
Dy2−O13−Dy4	108.72(15)	Dy2−O16−Dy4	106.74(15)
Dy3−O14−Dy4	110.11(15)	Dy3−O16−Dy4	108.51(15)

[a] Symmetry operations: a, 5/4−*x*, 1/4−*y*, *z*; c, 5/4−*x*, *y*, 1/4−*z*.

interactions between the metal centers induced by the hydroxido bridges. It is well-known for other metal ions linked by μ-OH^- ligands that the M−O−M angles have a great influence on the magnetic exchange coupling.[62−66] One can rationally expect the same effect for the Dy−O−Dy angles. Indeed, the Dy−O−Dy angle will modify the overlap between the magnetic orbitals of the Dy ions and therefore will influence the intracubane magnetic interactions, although such intra and intercubane interactions are expected to be very weak. Moreover, the local tensor of anisotropy on each Dy site and their relative orientations caused by the change of Dy−O−Dy angle could be a crucial feature to induce or not a SMM behavior in these

(62) Ruiz, E.; Alemany, P.; Alvarez, S.; Cano, J. *Inorg. Chem.* **1997**, *36*, 3683–3688.
(63) Ruiz, E.; Alemany, P.; Alvarez, S.; Cano, J. *J. Am. Chem. Soc.* **1997**, *119*, 1297–1303.
(64) Canada-Vilalta, C.; O'Brien, T. A.; Brechin, E. K.; Pink, M.; Davidson, E. R.; Christou, G. *Inorg. Chem.* **2004**, *43*, 5505–5521.
(65) Crawford, V. H.; Richardson, H. W.; Wasson, J. R.; Hodgson, D. J.; Hatfield, W. E. *Inorg. Chem.* **1976**, *15*, 2107–2110.
(66) Merz, L.; Haase, W. *J. Chem. Soc., Dalton Trans.* **1980**, 875–879.

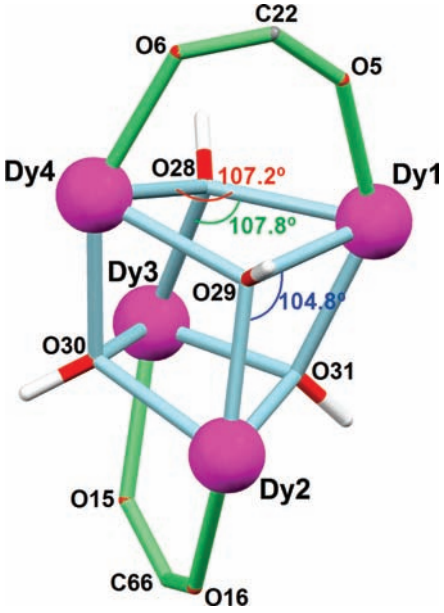

Figure 12. Cubane core of compound **2** showing characteristic M−O−M angles involving μ_3-hydroxido bridging ligands.

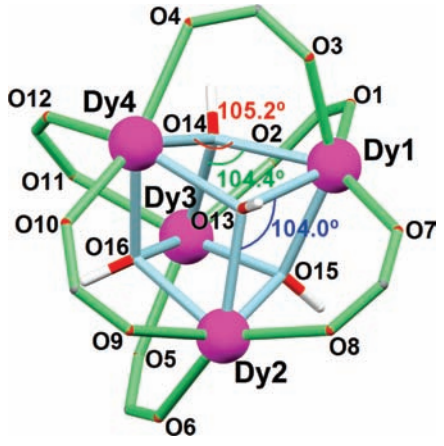

Figure 13. Cubane core of $[Dy_4(\mu_3\text{-}OH)_4(isonicotinate)_6(py)(CH_3OH)_7](ClO_4)_2\cdot py\cdot 4CH_3OH$(**3**)[44] showing characteristic M−O−M angles involving μ_3-hydroxido bridging ligands.

dysprosium systems.[67−69] In addition, the low symmetry of the Dy_4 cubane in compound **2** and their relative orientations may affect the cluster molecular anisotropy and hence lead to magnetization relaxation.[44] Actually, some of us have recently reported a tetranuclear dysprosium(III) compound, that is, $[Dy_4(\mu_3\text{-}OH)_4(isonicotinate)_6(py)(CH_3OH)_7](ClO_4)_2\cdot py\cdot 4CH_3OH$ (**3**),[44] whose cubane core (Figure 13) is structurally related to those herein described. This compound exhibits magnetic properties that are similar to that of bis-cubane **2**. In compound **3**, the Dy−O bonds are in the range 2.295(4)−2.407(4) Å.[44] The Dy−O−Dy angles of this cubane vary from 103.65(16) to 110.11(15)° (Table 4). Thus, the metric parameters for the cubane core of **3** (especially the Dy−O−Dy angles) are very close to those of compound **2**. In contrast to **1**, both **2** and **3** do not exhibit μ-hydroxido bridges that significantly alter the Dy−O−Dy angles. These features clearly suggest that the cubane angles together with the μ-OH^- bridge are responsible for the different magnetic behaviors observed.

Conclusions

In summary, two new Dy^{III} coordination compounds containing $[M_4O_4]$ cubane clusters have been prepared. The $[Dy_4(\mu_3\text{-}OH)_4]$ cubane cores of these two compounds exhibit a closely related structure. Nevertheless, the two Dy^{III} complexes possess distinct magnetic properties. While compound **1** does not show any out-of-phase ac signal, compound **2** exhibits slow relaxation of magnetization. A careful observation of the bond distances and angles of the respective $[Dy_4(\mu_3\text{-}OH)_4]$ cores reveals small but apparently crucial disparities in the M−O−M angles. These angle differences (induced by the presence of additional μ-OH^- bridges in **1**) clearly affect the orbital overlaps between the metal centers and the μ_3-hydroxido ligands, as well as the local tensor of anisotropy on each Dy site and their relative orientations, therefore generating dissimilar dynamic magnetic behavior. Theoretical studies are required to thoroughly analyze the Dy−O−Dy angle/magnetic property relationship.

Acknowledgment. J.T. thanks National Natural Science Foundation of China (Grants 20871113 and 20921002) for the financial support. P.G. acknowledges financial support from European Cooperation in the Field of Science and Technology (COST) Action D35/0011.

Supporting Information Available: Figures illustrating the coordination environments of the Dy^{III} ions in **1** and **2**; figures showing the crystal packings of **1** and **2**; hydrogen-bonding parameters for **1** and **2**; and additional magnetic data. This material is available free of charge via the Internet at http://pubs.acs.org.

(67) Ungur, L.; Van den Heuvel, W.; Chibotaru, L. F. *New J. Chem.* **2009**, *33*, 1224–1230.
(68) Luzon, J.; Bernot, K.; Hewitt, I. J.; Anson, C. E.; Powell, A. K.; Sessoli, R. *Phys. Rev. Lett.* **2008**, *100*, 247205.
(69) Chibotaru, L. F.; Ungur, L.; Soncini, A. *Angew. Chem., Int. Ed.* **2008**, *47*, 4126–4129.